**Supplementary Materials**

# Mitigating hydrogen evolution via ionomer structure for efficient $CO_2$ reduction in acidic membrane electrode assembly electrolyzers

**Zhongyin Kang[1,2], Min Zhang[1,2], Yang Wang[1,2], Qiang Liao[1,2], Qian Fu[1,2,*], Xun Zhu[1,2,*]**

[1]Key Laboratory of Low-grade Energy Utilization Technologies and Systems, Chongqing University, Ministry of Education, Chongqing 400044, China.
[2]Institute of Engineering Thermophysics, School of Energy and Power Engineering, Chongqing University, Chongqing 400044, China.

**Correspondence to:** Prof. Qian Fu, Prof. Xun Zhu, Institute of Engineering Thermophysics, School of Energy and Power Engineering, Chongqing University, Chongqing 400044, China. E-mail: fuqian@cqu.edu.cn; zhuxun@cqu.edu.cn

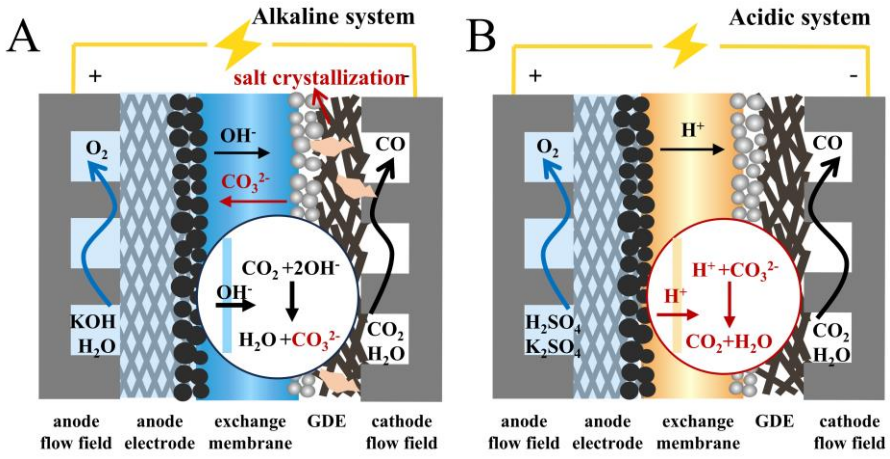


**Figure S1.** A–B: Schematic illustration of the carbonate/bicarbonate formation and crossover processes in alkaline and acidic media.

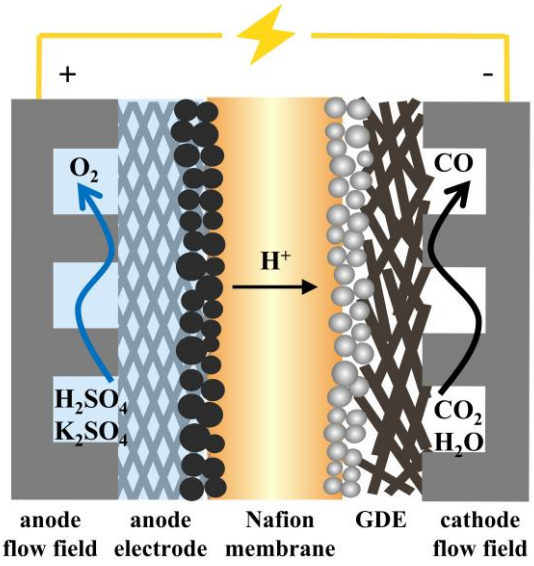


**Figure S2.** Schematic illustration of the MEA-type electrolyzer.

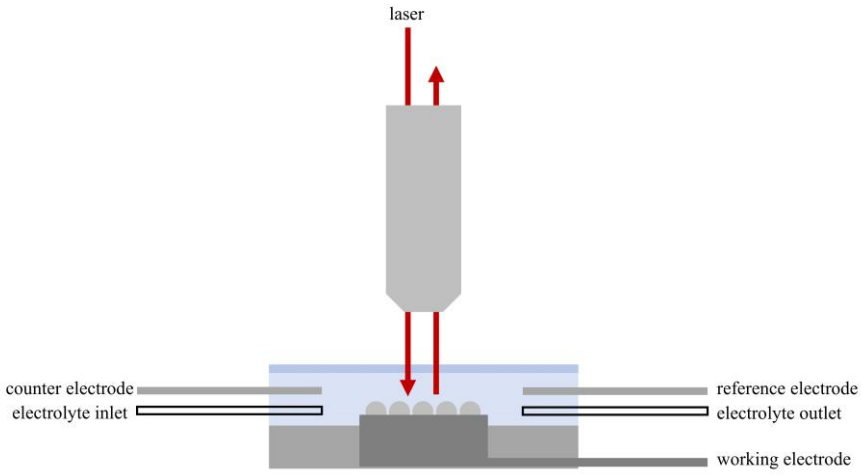


**Figure S3.** Schematic diagram of the in-situ ATR-SEIRAS device.

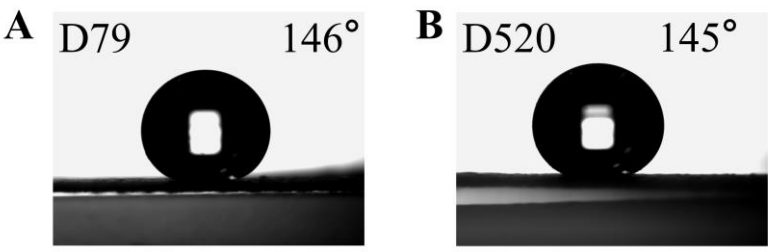


**Figure S4.** A: Water contact angle of D79; B: Water contact angle of D520.

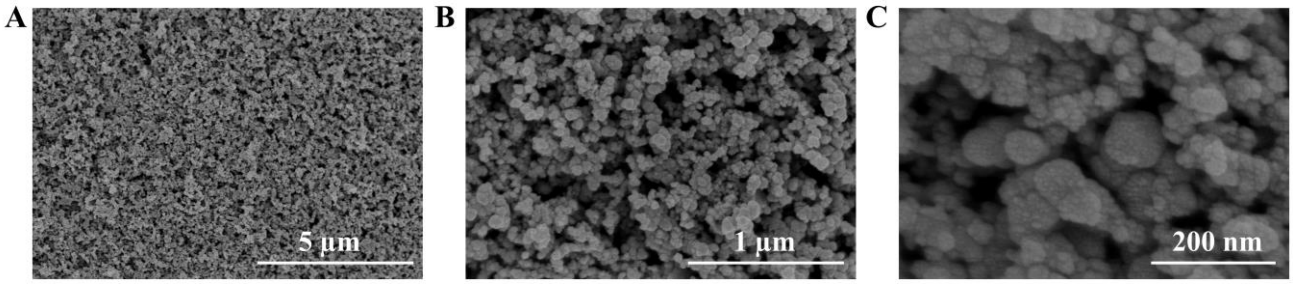


**Figure S5.** SEM images of GDE modified with LSC ionomer.

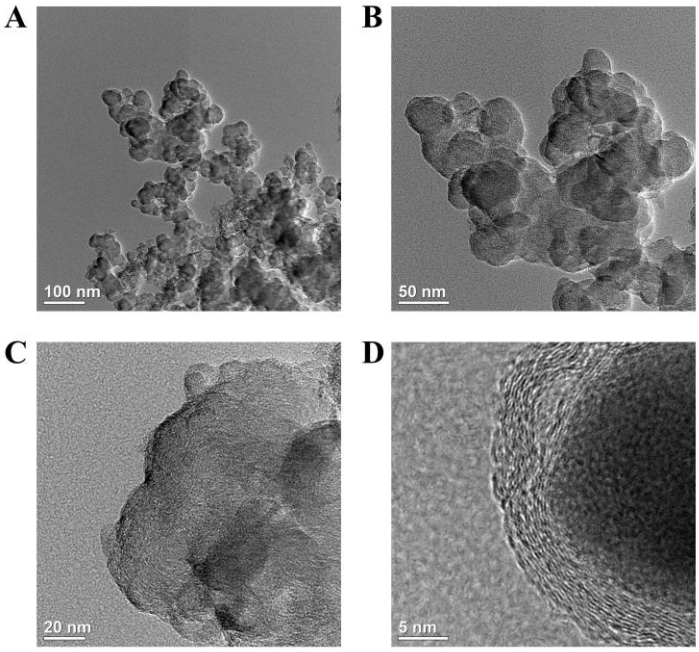


**Figure S6.** TEM images of GDE modified with LSC ionomer.

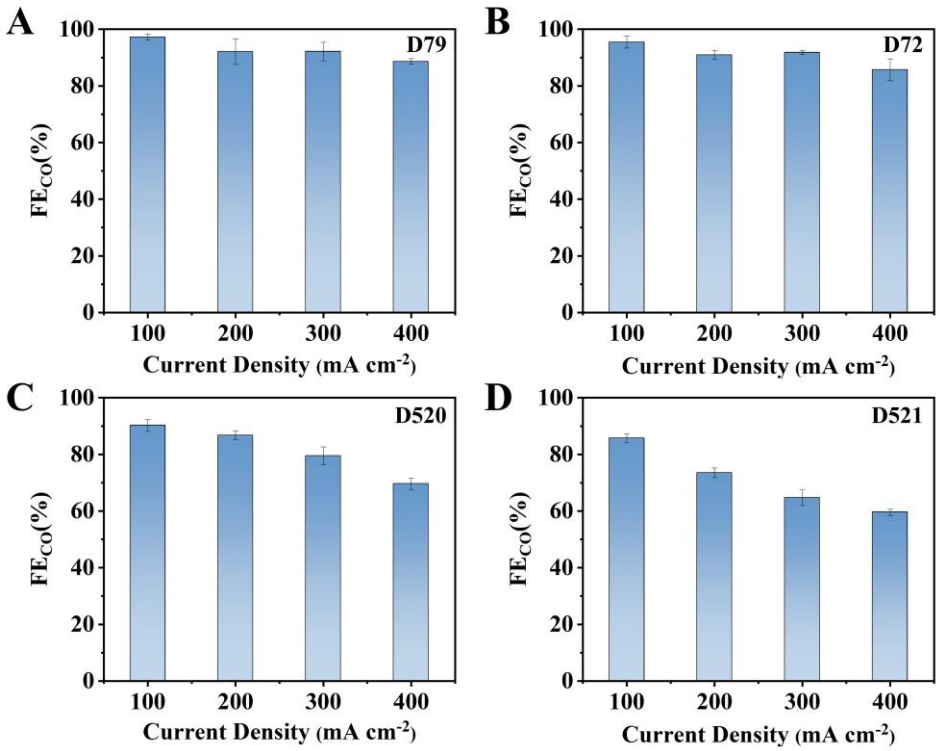


**Figure S7.** A–D: $FE_{CO}$ of GDEs with D79, D72, D520 and D521 at various current densities. Error bars represent the standard deviation from three independent measurements.

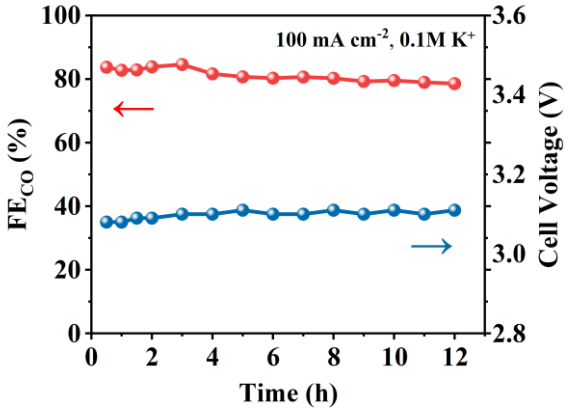


**Figure S8.** The long-term stability of the D79-modified Ni–N–C catalyst for acidic $CO_2$ electrolysis. The test was conducted at a current density of 100 mA cm$^{-2}$ in 0.05 M $K_2SO_4$ electrolyte with $H_2SO_4$ added to adjust the pH to 1. The red symbols and line represent the $FE_{CO}$, and the blue symbols and line represent the cell voltage.

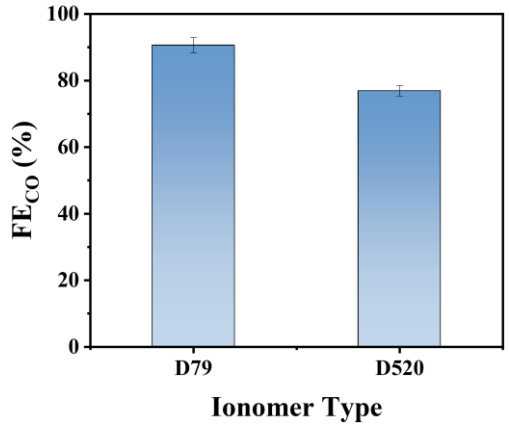


**Figure S9.** $FE_{CO}$ of Ag GDEs with different ionomers at 300 mA $cm^{-2}$. Error bars represent the standard deviation from three independent measurements.

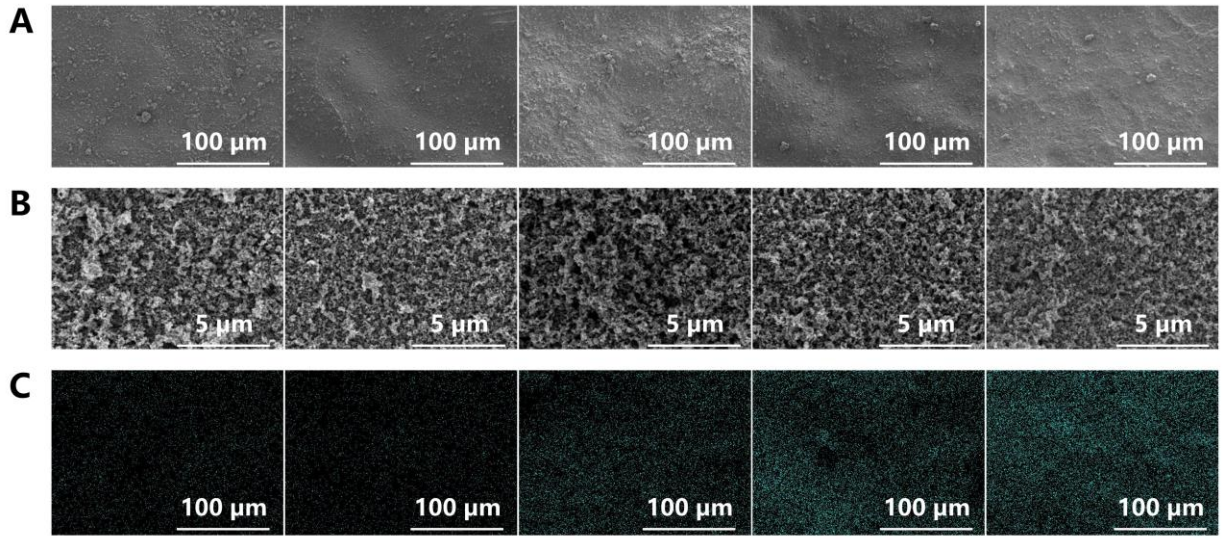


**Figure S10.** A–B: SEM images; C: Corresponding EDS images for F of GDEs with varying ionomer ratio (5%, 10%, 20%, 30% and 40%).

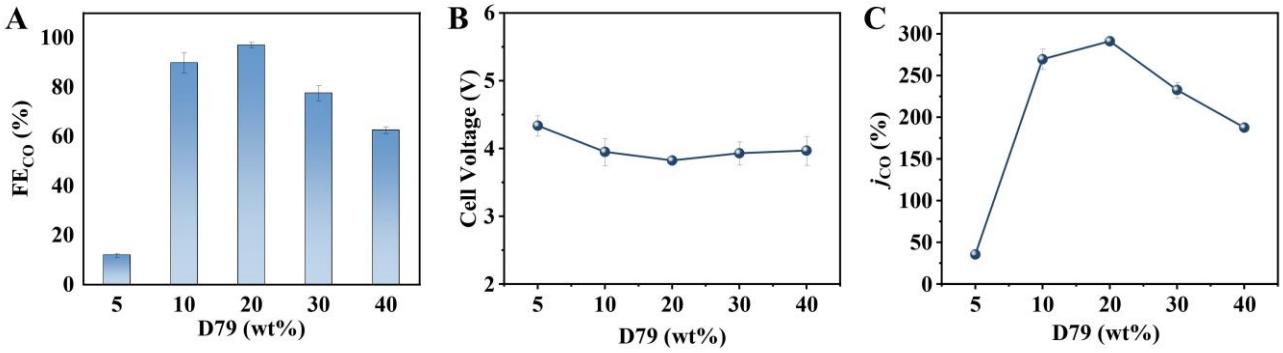


**Figure S11.** A: $FE_{CO}$, B: Cell voltage and C: $j_{CO}$ of GDEs with varying ionomer ratio at 300 mA $cm^{-2}$. Error bars represent the standard deviation from three independent measurements.

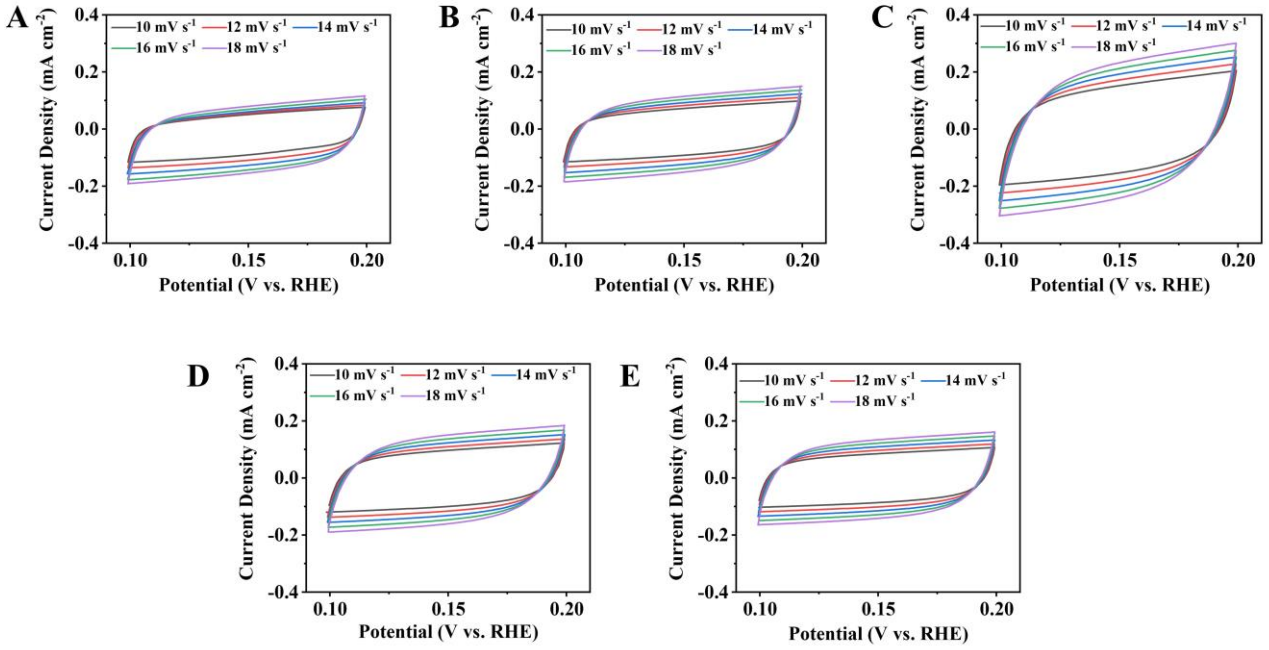


**Figure S12.** A–E: Capacitance measurements of GDEs with varying ionomer ratio (5%, 10%, 20%, 30% and 40%), measured from the CV at 0.1 V vs. RHE.

**Table S1.** Comparison of electrochemical performance with previously reported literature.

| | Current density (mA $cm^{-2}$) | $FE_{CO}$ (%) |
|---|---|---|
| This work | 500 | 91.1 |
| [1] | 100 | 90 |
| [2] | 60 | 80 |
| [3] | 250 | 90 |
| [4] | 6.5 | 89 |
| [5] | 500 | 85 |

**Table S2.** CO production rate ($r_{CO}$) and energy consumption ($E_{CO}$) of GDEs modified with D79 and D520 at various current densities.

| | D79 | | D520 | |
|---|---|---|---|---|
| Current density (mA $cm^{-2}$) | $r_{CO}$ (mmol $h^{-1}$ $cm^{-2}$) | $E_{CO}$ (kWh $kg^{-1}$) | $r_{CO}$ (mmol $h^{-1}$ $cm^{-2}$) | $E_{CO}$ (kWh $kg^{-1}$) |
| 100 | 1.81 | 6.04 | 1.68 | 6.61 |
| 200 | 3.44 | 7.29 | 3.24 | 8.04 |
| 300 | 5.16 | 7.82 | 4.45 | 9.29 |
| 400 | 6.61 | 8.39 | 5.20 | 11.04 |

The CO production rate ($r_{CO}$) was calculated as $r_{CO} = (I \times FE_{CO} \times 3600)/(2 \times F \times A)$, where I is the total current (A), $FE_{CO}$ is the Faradaic efficiency of CO (%), F is the Faraday constant (96485 C $mol^{-1}$), and A is the electrode area (1 $cm^2$). The energy consumption ($E_{CO}$) was calculated as $E_{CO}$

$=(U\times I\times t)/(n_{CO}\times 0.028)$, where U is the cell voltage (V), I is the total current (A), t is the electrolysis time (1 h), $n_{CO}$ is the molar amount of CO produced (mol), and 0.028 kg $mol^{-1}$ is the molar mass of CO. The unit of energy consumption is kWh $kg^{-1}$ CO [6].

## REFERENCES


[1] Monteiro M C O, Philips M F, Schouten K J P, et al. Efficiency and selectivity of $CO_2$ reduction to CO on gold gas diffusion electrodes in acidic media[J]. Nature communications, 2021, 12(1): 4943.

[2] Pan B, Fan J, Zhang J, et al. Close to 90% single-pass conversion efficiency for $CO_2$ electroreduction in an acid-fed membrane electrode assembly[J]. ACS Energy Letters, 2022, 7(12): 4224-4231.

[3] Sheng X, Ge W, Jiang H, et al. Engineering the Ni–N–C Catalyst Microenvironment Enabling $CO_2$ Electroreduction with Nearly 100% CO Selectivity in Acid[J]. Advanced Materials, 2022, 34(38): 2201295.

[4] Wang Z, Hou P, Wang Y, et al. Acidic electrochemical reduction of $CO_2$ using nickel nitride on multiwalled carbon nanotube as selective catalyst[J]. ACS Sustainable Chemistry & Engineering, 2019, 7(6): 6106-6112.

[5] Li H, Li H, Wei P, et al. Tailoring acidic microenvironments for carbon-efficient $CO_2$ electrolysis over a Ni–N–C catalyst in a membrane electrode assembly electrolyzer[J]. Energy & Environmental Science, 2023, 16(4): 1502-1510.

[6] Bard A J, Faulkner L R, White H S. Electrochemical Methods: Fundamentals and Applications[M]. John Wiley & Sons, 2022.